and HNA, respectively. The ratio of these lengths is very close to 3:4 and accounts for the compositionally invariant peak at $d \cong 2.1$ Å, which is the third order of 6.35 Å and the fourth order of 8.37 Å. Consequently, when two chains are in register at one point, there is between a 1 in 3 and a 1 in 4 chance (depending on the monomer ratio) that the ester oxygens of other individual monomers on the two chains will be in register. The 3:4 ratio is not exact, but there is some flexibility in the chain, and the energy gains due to stacking of the aromatic units and better chain packing will probably serve as a driving force to optimize the registration as defined here. The strong $d \cong 2.1$ Å meridional is a common feature of the aromatic copolyesters and copolyamides that we have examined, and this type of registration is probably also present in systems with more than two types of monomers.

A further point is that even limited register with one monomer of each chain in a plane exceeds what is necessary to generate the characteristics of order in the observed data. Better agreement is obtained when the origin monomer has a normal distribution about the register plane, with a standard deviation of $\sigma = 2.0$ Å. To put this in perspective, the difference in monomer lengths is 2.02 Å, and the maximum possible origin shift is ~4 Å (i.e., approximately half the average monomer length) since anything more than this brings a neighboring residue closer to the register plane. The normal distribution means that 68% of the origins must be within ±2.0 Å of the register plane. In the completely nematic structure 50% of the chain origins (51.5% for the 30/70 copolymer treated here) would occur over this distance. Hence although we clearly have some requirement for register, the requirement is not great and can be achieved with a very small shift of the chain along the axis. There is no need to invoke large shifts of the chains that optimize the alignment of identical sequences, which in any case would be insufficient to account for the observed crystallinity and crystallite size. Nucleation of the crystals may well involve alignment of a few short homopolymer sequences or identical copolymer sequences, but thereafter, register is envisaged in the limited way defined above.

Acknowledgment. This research was supported by NSF Grant No. DMR84-17525 from the Polymer Program.

Registry No. (HBA)(HNA) (copolymer), 81843-52-9.

References and Notes

(1) Chivers, R. A.; Blackwell, J.; Gutierrez, G. A.; Stamatoff, J. B.; Yoon, H. In *Polymeric Liquid Crystals*; Blumstein, A., Ed.; Plenum: New York, 1985; p 153.
(2) Blackwell, J.; Gutierrez, G. A.; Chivers, R. A. In *Polymeric Liquid Crystals*; Blumstein, A., Ed.; Plenum: New York, 1985; p 167.
(3) Blackwell, J.; Gutierrez, G. A.; Chivers, R. A. *Macromolecules* **1984**, *17*, 1219.
(4) Viney, C.; Windle, A. H. *J. Mater. Sci.* **1982**, *17*, 261.
(5) Chivers, R. A.; Blackwell, J.; Gutierrez, G. A. *Polymer* **1984**, *25*, 435.
(6) Blackwell, J.; Gutierrez, G. A.; Chivers, R. A.; Biswas, A. *J. Macromol. Sci., Phys.* **1985–1986**, *B24*(1–4), 39.
(7) Gutierrez, G. A.; Blackwell, J. *Macromolecules* **1984**, *17*, 2744.
(8) Biswas, A.; Blackwell, J. *Macromolecules* **1987**, *20*, 2997.
(9) Calundann, G. W.; Jaffe, M. *Proc. Robert A. Welch Found. Conf. Chem. Res. 26*, 247.
(10) Blackwell, J.; Cheng, H.-M.; Biswas, A. *Macromolecules* **1988**, *21*, 39.
(11) Blackwell, J.; Biswas, A.; Gutierrez, G. A.; Chivers, R. A. *Faraday Discuss. Chem. Soc.* **1985**, *No. 79*, 73.
(12) Butzbach, G. D.; Wendorff, J. H.; Zimmermann, H. J. *Polymer* **1986**, *27*, 1337.
(13) Butzbach, G. D.; Wendorff, J. H.; Zimmermann, H. J. *Makrolmol. Chem., Rapid Commun.* **1985**, *6*, 821.
(14) Chivers, R. A.; Blackwell, J. *Polymer* **1985**, *26*, 997.
(15) Biswas, A.; Blackwell, J. *Macromolecules*, companion papers in this issue.
(16) Geiss, R. H.; Street, G. B.; Volksen, W.; Economy, J. *IBM J. Res. Dev.* **1983**, *27*(4), 321.
(17) Northolt, M. S. *Eur. Polym. J.* **1974**, *10*, 799.
(18) Windle, A. H.; Viney, C.; Golombok, R.; Donald, A. M.; Mitchell, G. R. *Faraday Discuss. Chem. Soc.* **1985**, *No. 79*, 55.
(19) Hanna, S.; Windle, A. H. *Polymer* **1988**, *29*, 207.
(20) Blackwell, J.; Biswas, A.; Bonart, R. C. *Macromolecules* **1985**, *18*, 2126.
(21) Keller, A.; Maradudin, A. *J. Phys. Chem. Solids* **1957**, *2*, 301.
(22) Gutierrez, G. A.; Chivers, R. A.; Blackwell, J.; Stamatoff, J. B.; Yoon, H. *Polymer* **1983**, *24*, 937.

Three-Dimensional Structure of Main-Chain Liquid-Crystalline Copolymers. 3. Chain Packing in the Solid State

Amit Biswas and John Blackwell*

Department of Macromolecular Science, Case Western Reserve University, Cleveland, Ohio 44106-2699. *Received December 15, 1987*

ABSTRACT: This paper describes the three-dimensional structure for the ordered packing of wholly aromatic thermotropic copolyesters. Previous work has established that copolyesters prepared, e.g., from *p*-hydroxybenzoic acid (HBA) and 2-hydroxy-6-naphthoic acid (HNA) are random copolymers, based on the observed aperiodicity of the meridional diffraction maxima. However, the presence of sharp equatorial and off-equatorial Bragg maxima is indicative of three-dimensional order akin to crystallinity. In the as-spun fibers, there is orthorhombic (pseudohexagonal) packing of the chains, with a base plane unit cell with dimensions $a = 9.18$ Å and $b = 5.30$ Å. Paper 1 of the series in this issue established that in order to generate the first layer line the chains must have a pseudodimer repeat; i.e., there are conformational correlations between adjacent monomers along the chain. Paper 2 showed that the off-equatorial Bragg maxima are generated by limited axial register between adjacent random sequences. In the present paper, we consider the actual conformation and packing of the chains. Analyses are developed to predict the diffraction patterns of assemblies of random sequences, with varying degrees of rotational correlations between dimer units on adjacent chains. The results show a preference for a chain conformation in which aromatic planes along the chain are mutually inclined at ~60°, in a structure analogous to that of poly(*p*-phenyleneterephthalamide). The conformational correlations of the dimers along adjacent chains are quite limited; i.e., the three-dimensional "crystallinity" corresponds to regions of local order that probably arise due to the anisotropic cross sections of the monomer units.

Introduction

This paper extends our previous X-ray analyses of the structure of wholly aromatic copolyesters to look at the chain conformation and packing in the solid state. At the present time, there is considerable interest in the structure–property relationships of copolyesters prepared from,

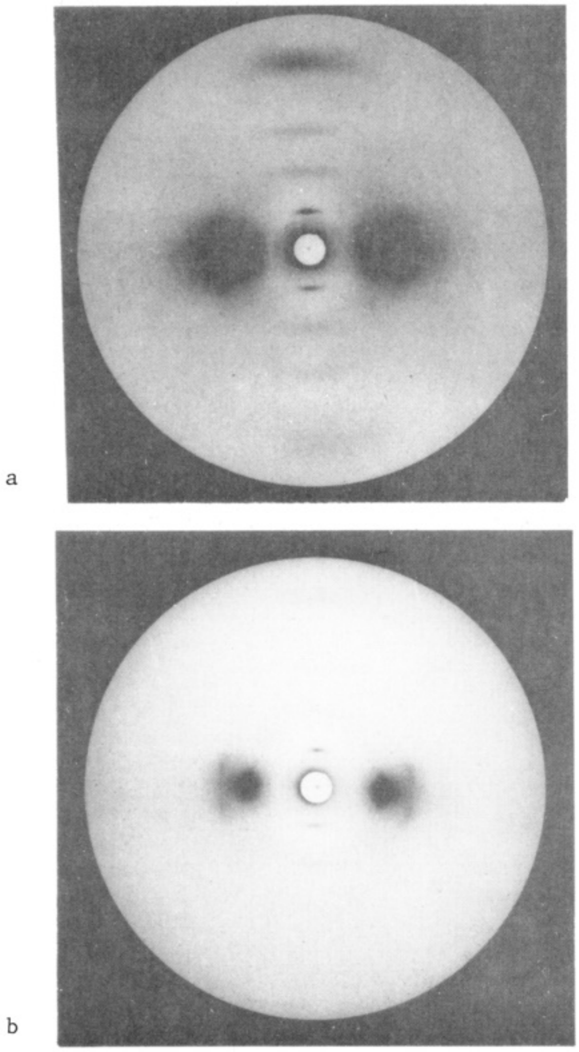

Figure 1. Fiber diffraction patterns from melt-drawn samples of 30/70 copoly(HBA/HNA) at (a) high-exposure and (b) low-exposure times.

e.g., *p*-hydroxybenzoic acid (HBA) and 2-hydroxy-6-naphthoic acid (HNA) or from HBA, biphenol (BP), and terephthalic acid (TPA). Typically these monomers are copolymerized in the melt via acetolysis. Our previous X-ray analyses have shown that these are random copolymers, as has been confirmed in other laboratories.[1-4] This conclusion is derived from the aperiodic intensity distribution along the meridian of the fiber diagrams, which arises due to structural correlations in the relatively stiff extended chains of random sequence. Nevertheless, the X-ray patterns contain sharp Bragg diffraction maxima that are indicative of crystallinity; i.e., there is three-dimensional order despite the random sequence and the dissimilarity of the component monomers. Paper 1 of the series in this issue[5] addressed the X-ray scattering at the level of a single chain and discussed the possible chain conformation. Thereafter, the interference effects for arrays of random copolymer chains in register were derived in paper 2.[6] We are now able to extend our analyses to consider the actual chain packing in these arrays.

Figure 1 shows the X-ray fiber diagram for melt-spun fibers of 30/70 copoly(HBA/HNA). The meridian shows four intensity maxima at $d = 7.89$, 4.09, 2.89, and 2.1 Å, which are reproduced in position in the scattering pattern calculated for a nematic array of infinite chains of completely random comonomer sequence.[7,8] The calculation also gives good agreement with the observed intensities of the maxima, except for the first peak at $d = 7.89$ Å, which is predicted to be weaker than that observed. Better agreement is obtained when the proposed structure is modified from that of a nematic to a situation where there is limited chain register.[6] A further point is that the maximum at $d = 2.1$ Å is predicted to be much sharper (along the meridian) than that observed. The predicted width is increased to match that observed when we consider shorter chains or allow for nonlinearity in the chain conformation. We have introduced the concept of a solid-state correlation length to describe this conformational nonlinearity, which for as-spun specimens is typically ~80 Å, corresponding to about 11 monomers in chain length.[9]

The evidence for three-dimensional order comes from the existence of equatorial and off-equatorial Bragg reflections. In the as-spun state, three equatorials are seen at $d = 4.6$, 2.6, and 2.3 Å, which can be indexed as the 100, 110, and 200 reflections, respectively, for a two-dimensional hexagonal unit cell with dimension $a = 5.3$ Å. (These *d*-spacings are for 30/70 copoly(HBA/HNA). Those for equatorials for the other comonomer ratios are the same within experimental error). On the basis of density and molecular dimensions, this unit cell would contain one copolymer chain. In addition to the equatorials, a single off-equatorial is seen at $d = 3.3$ Å, and it is the presence of this reflection that requires some form of three-dimensional registration of the chains. The reciprocal space coordinates of this maximum (for the 30/70 copolymer) are $R,Z = 0.294, 0.067$ Å^{-1}. This maximum is not indexed by the one-chain unit cell but requires conversion to the two-chain pseudohexagonal option with $a = 9.18$ Å and $b = 5.3$ Å. In this case the equatorials index as 110/200, 020/310, and 220/400, and R for the off-equatorial is indexed by $h = 2$ and $k = 1$. For convenience we will refer to the off-equatorial as the 211 reflection since it occurs on the first aperiodic layer line.

In order to determine the three-dimensional structure of the copolymer, it is necessary to consider first the actual chain conformation and then the way in which such chains are packed in an ordered manner. The scattering on the meridian derives from the projection of the structure onto the fiber axis, which is largely independent of the chain conformation, due to the fact that the aromatic linkage bonds are approximately parallel to the chain axis. To expand these analyses to three dimensions, it is necessary to consider the conformational correlation of one monomer to the next along the chain. A key observation is that the 211 reflection lies on the layer line at $Z = 0.067$ Å^{-1}, approximately half that for the first meridional at $Z = 0.127$ Å^{-1}. Paper 1[5] showed that this imposes a pseudodimer repeat on the copolymer, analogous to the dimer repeats seen for homopoly(HBA) and poly(*p*-phenyleneterephthalamide). The present paper will examine the actual conformation during refinement of the structure.

The question of registration of the random copolymer sequences was addressed in paper 2,[6] where we showed that the diffraction characteristics associated with three-dimensional crystallinity are generated if we require an origin atom on each chain to lie about a register plane perpendicular to the chain axis. This is a more "liberal" definition of chain register than has been proposed by Viney and Windle,[10,11] who have suggested that the three-dimensional order arises due to segregation of identical sequences. Even if such segregation could occur on quenching, it is unlikely that it would generate the relatively high crystallinities and lateral crystallite sizes that have been reported.[12] Our definition of register requires axial shifts of ~4 Å or less and aligns completely random sequences.

Furthermore, this model predicts Bragg sampling on all layer lines, whereas they only occur on the first-layer line for as-spun specimens. To reproduce the observed characteristics, it is necessary to relax the registration condition: rather than requiring the origin monomer to lie *on* the register plane, there is a normal distribution *about* the plane. The standard deviation, σ, for this distribution is $\sim$2.0 Å, which is approximately the difference in length between the HBA and HNA residues. This gives some idea of how minimal is the registration in the as-spun state of copoly(HBA/HNA). Higher layer lines are seen for annealed specimens of this copolymer, which indicates that registration can be improved, corresponding to a decrease in σ.

The above analyses of the three-dimensional structure were done for an assembly of 200 chains by using the one-chain unit cell. The chain conformation used was the so called "random dimer" model. Rigid models for the four possible dimers were linked in random sequences, and there was no torsional correlation between adjacent dimers: this was achieved by cylindrical averaging of each dimer in real space before calculation of the intensity transform, which was then sampled by the interference function for chain packing. The reflections predicted on the first-layer line do not include the one observed because of the use of a one-chain unit cell, but the results are sufficient to show that the diffraction effects are generated with limited register.

In the present paper, we consider the actual chain packing in the ordered structure. The existence of a two-chain unit cell requires structural differences between the adjacent chains. We have extended our previous analyses to consider an assembly of chains in which the dimers on adjacent chains are fixed rather than cylindrically averaged. The monomer orientation and stagger of adjacent chains have been adjusted in order to refine the conformation and packing.

Diffraction by Ordered Regions in Fibers

We have shown previously in paper 2[6] that the interference function for a parallel bundle of M finite chains can be written as

$$I(R,Z) = MI_a(R,Z) + A(Z)\ I_b(R,Z)\ I_c(R) \qquad (1)$$

where $I_a(R,Z)$ and $I_b(R,Z)$ are the intra- and interchain interferences, respectively. $A(Z)$ is the distribution function describing axial register, and $I_c(R)$ is the interference function on the basal plane attributed to the packing arrangement.

The above separation of the $I_b(R,Z)$ and $I_c(R)$ terms in the total interchain interference is possible only when there are no rotational correlations between residues on adjacent chains. When we have fixed positions for residues on adjacent chains, the (cylindrically averaged) interference for an ordered region consisting of N atoms can be written as[13]

$$I_{\mathrm{ord}}(R,Z) = \sum_{j=1}^{N} \sum_{k=1}^{N} f_j f_k J_0(2\pi R r_{jk}) \exp(2\pi i Z z_{jk}) \qquad (2)$$

where r_{jk} is the projected distance on the basal ($z = 0$) plane between the jth and kth atom and z_{jk} is the corresponding projected distance along the fiber (z) axis. J_0 represents the zeroth-order Bessel function. r_{jk} can be further expressed in terms of the interchain and intrachain components as

$$r_{jk} = (r_{mm'}^2 + r_{kk'}^2 - 2r_{mm'}r_{kk'} \cos \phi_{mm'kk'})^{1/2} \qquad (3)$$

where mm' and kk' represent the inter- and intrachain vectors, respectively, and $\phi_{mm'kk'}$ is the angle between the mm' and kk' vectors. Since

$$J_0(a) = J_0(b)\ J_0(c) + 2\sum_{n=1}^{\infty} J_n(b)\ J_n(c) \cos n\phi \qquad (4)$$

when $a^2 = b^2 + c^2 - 2bc \cos \phi$, $I_{\mathrm{ord}}(R,Z)$ can be written as

$$I_{\mathrm{ord}}(R,Z) = \sum_{m}\sum_{m'}\sum_{k}\sum_{k'} f_k f_{k'} J_0(2\pi R r_{mm'})\ J_0(2\pi R r_{kk'}) \times \exp[2\pi i Z(z_{k'} - z_k)] + 2\sum_{n=1}^{\infty}\sum_{m}\sum_{m'}\sum_{k}\sum_{k'} f_k f_{k'} J_n(2\pi R r_{mm'}) \times J_n(2\pi R r_{kk'}) \exp[2\pi i Z(z_{k'} - z_k)] \cos (n\phi_{mm'kk'}) \qquad (5)$$

When $m = m'$, eq 5 describes the intrachain interference function; $m \neq m'$ represents the interchain interference. In the case of the random copolymer, when there are no correlations for rotations of the residues about the chain axis, the total interchain interference function (the second term in eq 1) is given by

$$I_2(R,Z) = A(Z)\ I_b(R,Z)\ I_c(R) \qquad (6)$$

where

$$I_b(R,Z) = \mathrm{Re} \sum_{\mathrm{A}}\sum_{\mathrm{B}} F_{\mathrm{AB}}(R,Z)[U_{\mathrm{AB}}(Z) + 2V_{\mathrm{AB}}(Z)] \qquad (7)$$

$$I_c(R) = \sum_{m}\sum_{m'} J_0(2\pi R r_{mm'}); \qquad m \neq m' \qquad (8)$$

and

$$F_{\mathrm{AB}}(R,Z) = \sum_{j}\sum_{k} f_{\mathrm{A},j} f_{\mathrm{B},k} J_0(2\pi R r_{\mathrm{A},j})\ J_0(2\pi R r_{\mathrm{B},k}) \exp[2\pi i Z(z_{\mathrm{B},k} - z_{\mathrm{A},j})] \qquad (9)$$

Here, $F_{\mathrm{AB}}(R,Z)$ is the Fourier transform of the cross convolution of residue A with residue B *after* each has been cylindrically averaged in real space. $U_{\mathrm{AB}}(Z)$ and $V_{\mathrm{AB}}(Z)$ are matrices of interference terms, as defined in paper 2,[6] arising from interactions between corresponding and noncorresponding residues on different chains, respectively. That is to say, the components of $U_{\mathrm{AB}}(Z)$ originate from the interference between the nth residue of chain i and the nth residue of chain j, while those of $V_{\mathrm{AB}}(Z)$ arise from the interference between the mth residue of chain i and the nth residue ($m \neq n$) of chain j. The influence of these terms on the extent of order will be discussed later on. When definite correlations between residues of different chains in the crystallite are imposed, $F_{\mathrm{AB}}(R,Z)$ has to be replaced by $F'_{\mathrm{AB}}(R,Z)$, which incorporates $I_c(R)$

$$F'_{\mathrm{AB}}(R,Z) = 2\sum_{n=0}^{\infty}{}'\sum_{m}\sum_{m'}\sum_{j}\sum_{k} f_{\mathrm{A},j} f_{\mathrm{B},k} J_n(2\pi R r_{mm'}) \times J_n(2\pi R r_{\mathrm{A},j\mathrm{B},k}) \exp[2\pi i Z(z_{\mathrm{B},k} - z_{\mathrm{A},j})] \cos [n(\phi_{mm'} - \phi_{\mathrm{A},j\mathrm{B},k})] \qquad (10)$$

The prime in the summation over n indicates that only half weight is given to $n = 0$, and the subscripts A,j and B,k represent the jth atom of monomer A and the kth atom of monomer B, respectively. The terms in $F'_{\mathrm{AB}}(R,Z)$ can be grouped for convenience into intra- and interchain components

$$F'_{\mathrm{AB}}(R,Z) = 2\sum_{n=0}^{\infty} [R_n(R)\ A_{n,\mathrm{AB}}(R,Z) + S_n(R)\ B_{n,\mathrm{AB}}(R,Z)] \qquad (11)$$

where

$$A_{n,\mathrm{AB}}(R,Z) = \sum_{j}\sum_{k} f_{\mathrm{A},j} f_{\mathrm{B},k} J_n(2\pi R r_{\mathrm{A},j\mathrm{B},k}) \exp[2\pi i Z(z_{\mathrm{B},k} - z_{\mathrm{A},j})] \cos (n\phi_{\mathrm{A},j\mathrm{B},k}) \qquad (12)$$

$S_n(R)$ and $B_{n,\mathrm{AB}}(R,Z)$ are the corresponding sine components. Figure 2 shows a pseudohexagonal lattice in which the center chains are shaded to indicate that they are different from the corner chains. This structure can be

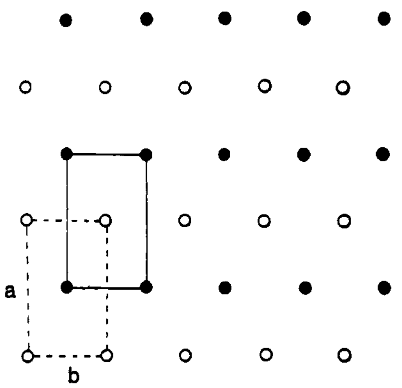

Figure 2. Hexagonal lattice comprised of two interpenetrating orthorhombic lattices of the corner chains and the center chains.

viewed as two interpenetrating primitive lattices, one composed of the center chains and the other of the corner chains, each with dimensions $a = 9.18$ Å and $b = 5.3$ Å. Following the derivations in paper 2,[6] the interference function $I_c(R)$ can be divided into components which represent the interference from each individual primitive lattice, $I_{11}(R)$, and the interference between the two interpenetrating lattices, $I_{12}(R)$, respectively.

$$I_c(R) = I_{11}(R) + I_{12}(R) \tag{13}$$

$$I_{11}(R) = 4 \sum_{p=0}^{M_1-1}{}' \sum_{q=0}^{M_2-1}{}'(M_1 - p)(M_2 - q)J_0[2\pi R(p^2a^2 + q^2b^2)^{1/2}] \tag{14}$$

$$I_{12}(R) = 4 \sum_{p=0}^{M_1-1} \sum_{q=0}^{M_2-1} [M_1 - (p + ½)][M_2 - (q + ½)]\ J_0[2\pi R((p + ½)^2a^2 + (q + ½)^2b^2)^{1/2}] \tag{15}$$

M_1, M_2, a, and b are now defined in terms of the individual primitive lattices, i.e., $M_1 = M_2 = 10$, $a = 9.18$ Å, and $b = 5.3$ Å. In this context

$$R_n(R) = 4 \sum_{p=0}^{M_1-1}{}' \sum_{q=0}^{M_2-1}{}'(M_1 - p)(M_2 - q)J_n[2\pi R(p^2a^2 + q^2b^2)^{1/2}] \cos (n\phi_{11}) + 4 \sum_{p=0}^{M_1-1} \sum_{q=0}^{M_2-1} [M_1 - (p + ½)][M_2 - (q + ½)]\ J_n[2\pi R((p + ½)^2a^2 + (q + ½)^2b^2)] \cos (n\phi_{12}) \tag{16}$$

where

$$\phi_{11} = \tan^{-1} (qb/pa)$$
$$\phi_{12} = \tan^{-1} [(q + ½)b/(p + ½)a]$$

The total interchain interference, $I_2(R,Z)$, can now be expressed in a manner which indicates the extent of rotational correlations between dimers on different chains:

$$I_2(R,Z) = A(Z)\ I_{bc}(R,Z) \tag{17}$$

Three cases are considered for $I_{bc}(R,Z)$.

if there are no correlations between any dimers:

$$I_{bc}(R,Z) = (\mathrm{Re} \sum_{\mathrm{A}}\sum_{\mathrm{B}} F_{\mathrm{AB}}(R,Z)[U_{\mathrm{AB}}(Z) + 2V_{\mathrm{AB}}(Z)])I_c(R) \tag{18}$$

for rigid rotational correlations between all dimers:

$$I_{bc}(R,Z) = \mathrm{Re} \sum_{\mathrm{A}}\sum_{\mathrm{B}} F'_{\mathrm{AB}}(R,Z)[U_{\mathrm{AB}}(Z) + 2V_{\mathrm{AB}}(Z)] \tag{19}$$

for rotational correlations only between corresponding dimers on all chains:

$$I_{bc}(R,Z) = \mathrm{Re} \sum_{\mathrm{A}}\sum_{\mathrm{B}} [F'_{\mathrm{AB}}(R,Z)\ U_{\mathrm{AB}}(Z) + 2F_{\mathrm{AB}}(R,Z)\ V_{\mathrm{AB}}(Z)\ I_c(R)] \tag{20}$$

The separability of $I_b(R,Z)$ (eq 7) into $F_{\mathrm{AB}}(R,Z)$, $U_{\mathrm{AB}}(Z)$, and $V_{\mathrm{AB}}(Z)$ is quite important if we are to introduce different degrees of order into the array of chains, as will be discussed further.

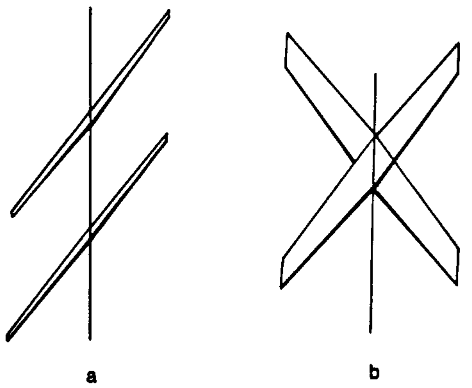

Figure 3. *ab* projection of the HBA dimer with (a) parallel aromatic planes and (b) inclined aromatic planes.

Experimental Section

Models for the copoly(HBA/HNA) chain were constructed as random arrays of the four possible dimers. Two different models were considered for each dimer.

(a) The first was a pseudo 2_1 screw axis conformation in which the torsion angles Φ_1,Φ_2 between the aromatic and ester groups are alternately 30°,–30° and 150°,–150°. This results in parallel aromatic planes which are inclined to the ester planes by 30°, analogous to the proposed structure of homopoly(HBA).[14]

(b) The second was a conformation analogous to that in poly(*p*-phenyleneterephthalamide)[15] with Φ_1,Φ_2 alternately 30°,30° and 150°,150°. The aromatic planes are inclined at 60° with respect to each other; the ester planes are parallel and inclined at 30° to the aromatic planes. These conformations for an HBA dimer are shown in Figure 3 and will be refered to as the parallel aromatic and inclined aromatic conformation, respectively.

Two hundred dimers were arranged as shown in Figure 4. This structure can be thought as a slice one dimer thick taken perpendicular to the fiber axis. Calculations were done for structures consisting exclusively of one of the four dimers, with every lattice point occupied by a composite of the four dimers, each weighted according to its occurrence in the 30/70 copolymer. All dimers were set with their initial ester oxygen atoms in the register plane. $F'_{\mathrm{AB}}(R,Z)$ was calculated at $Z = 0.067$ Å^{-1}, corresponding to the position of the first layer line in the fiber diagram. The center and corner units had different orientations that were related by symmetry operations as follows:

(a) Center and corner chains have the same (parallel) sense, and the equivalent positions are x, y, z and $0.5 - x, 0.5 + y, z$ for both conformations.

(b) Center and corner chains have opposite (antiparallel) sense, in which case the equivalent positions are x, y, z and $0.5 - x, 0.5 + y, -z$ for the parallel aromatic conformation and x, y, z and $0.5 + x, 0.5 + y, -z$ for the inclined aromatic conformation.

F'_{AB} (R, 0.067 Å^{-1}) was evaluated for the dimer slice at 201 equally spaced sampling points between $R = 0$ and 0.5 Å^{-1}, using eq 11, incorporating orders of Bessel functions from $n = 0$ to 5. Inclusion of higher orders of n did not lead to significantly different results.

As will be seen in the Results and Discussion section, these calculations showed that the inclined aromatic conformation gives much better agreement with the observed diffraction data, and this conformation was used for the longer calculation for the array of copolymer chains. The array of 200 dimers considered above was extended to 200 chains of 15 dimers. Three structures were considered: (a) no rotational correlations whatsoever in the chain packing, (b) completely rigid chains with the inclined dimer conformation and full rotational correlations along the entire length of the chains, and (c) rigid correlations of dimers in a slice but no rotational correlations extending along the chain. $I(R$, 0.067 Å$^{-1})$ was calculated in 201 increments from $R = 0$ to 0.5 Å^{-1}. The best agreement was obtained for case (c) above, and the entire diffraction pattern $I(R,Z)$ was calculated for this structure, using a 201 × 201 R,Z grid out to $R = Z = 0.5$ Å^{-1} but limited to a

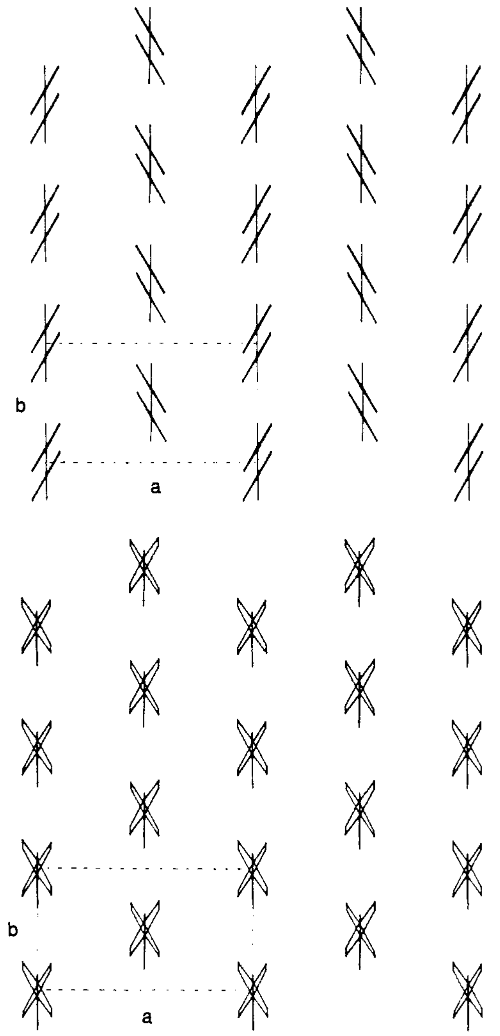

Figure 4. Portion of a layer of packed HBA dimers with (a, top) parallel aromatic planes and (b, bottom) inclined aromatic planes.

scattering angle of $2\theta = 50°$ ($\theta = \sin^{-1}(\lambda/2(R^2 + Z^2)^{1/2})$).

Results and Discussion

Figure 5 shows the calculated intensity on the first layer for homopoly(HBA) in two different conformations, derived from the calculation for the layer of HBA dimers all with parallel sense. It can be seen that the inclined aromatic conformation leads to high intensity for the 211 reflection and weaker intensity for the neighboring 111/201 reflection, whereas the reverse is the case for the parallel aromatic conformation. Similar results are obtained by using antiparallel chain packing, and it appears that conformation and stagger are more important determinants of the X-ray scattering than chain sense. This is expected since the ester groups are minor components of the structure compared to the aromatic units. Also, the X-ray data for copoly(HBA/HNA) are very similar to those for copolyesters that have no chemical sense, such as copoly(HBA/BP/TPA).[16] The strong intensity for the 211 reflection and the absence of *hkl* reflections with $h + k + l$ odd are indicative of an approximate body-centered relationship between monomers in the unit cell. This occurs in the structure in Figure 4b for the packing of the inclined aromatic conformation but not for the parallel aromatic conformation, Figure 4a. Similar results are obtained for structures made up exclusively of the other three types of dimers. Figure 6 shows the results for the structure with an average dimer at each lattice point, again with parallel chain sense. The results are similar to those in Figure 5 in that the inclined aromatic conformation leads to a strong 211 reflection compared to weaker neighbors, with the reverse effect occurring for the parallel aromatic conformation. The differences are less clear-cut than for homopoly(HBA) but can be enhanced by refinement of the chain orientation and stagger. We conclude that the inclined aromatic conformation is the more likely of the two, and this is used for further analysis of the structure when longer chains are considered.

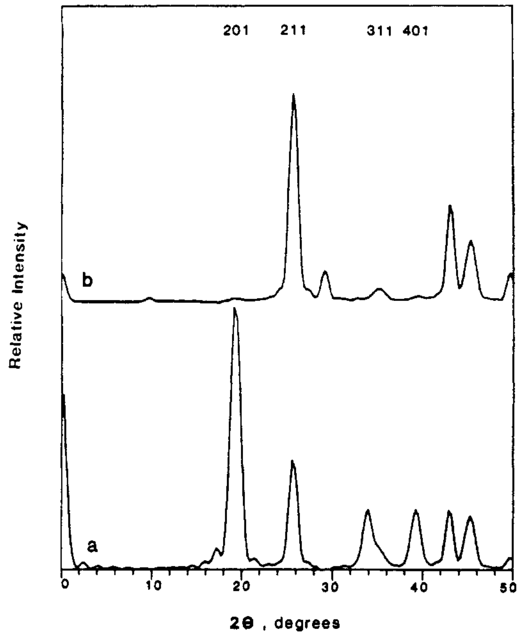

Figure 5. Intensity distribution on the first-layer line ($Z = 0.079$ Å^{-1}) calculated for a layer of 200 HBA dimers (a) arranged as shown in Figure 4a and (b) arranged as shown in Figure 4b.

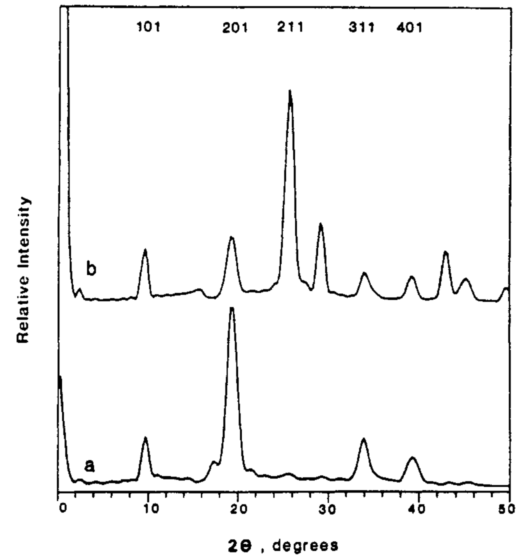

Figure 6. Intensity distribution on the first-layer line ($Z = 0.067$ Å^{-1}) calculated for a layer of averaged dimers of 30/70 copoly(HBA/HNA) with (a) parallel aromatic planes and (b) inclined aromatic planes.

Figure 7 shows the predicted first-layer line intensities for structures consisting of 200 random chains, each of 15 dimers. Each lattice point is occupied by an average chain, with its origin ester oxygen in the register plane. Curve a is obtained for a structure in which there are no rotational correlations between successive rigid dimers, i.e., when there is a cylindrically averaged chain at each lattice point. In this case we have hexagonal packing of the chains in register, and the predicted first layer line shows peaks only for $h + k$ even, i.e., 111, 201, and 221: there is no 211

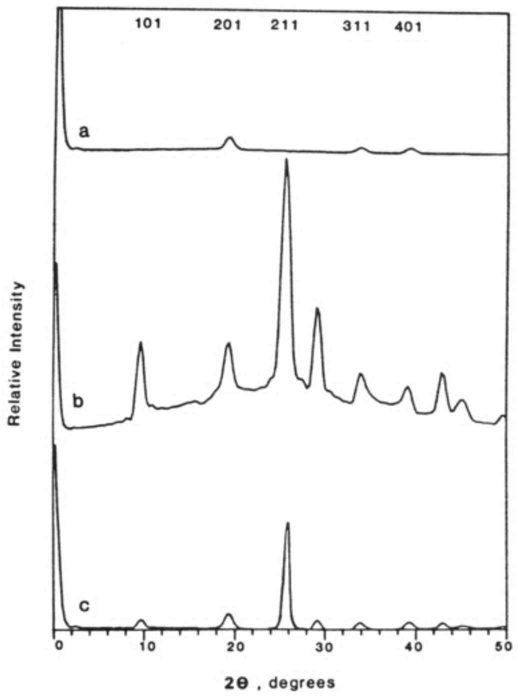

Figure 7. Comparison of the intensity distribution on the first-layer line ($Z = 0.067$ Å^{-1}) calculated for 200 chains of 30/70 copoly(HBA/HNA) with (a) no correlations between any dimers, (b) rigid correlations between all dimers, and (c) rotational correlations only between corresponding dimers on all chains.

reflection. Curve b shows the results for a structure made up of rigid chains, where the inclined aromatic conformation repeats along the entire chain. The first-layer line contains a strong 211 peak, with weaker but significant peaks for even $h + k$. It should be noted that none of the latter occurs in the observed data. Furthermore, such extensive rigid correlations in the chain axis direction are unlikely in any real structure simply because of the problems of packing of the random sequences.

Curve c in Figure 7 is the first-layer line for a compromise structure with more limited rotational correlations between the dimers. The model used has no rotational correlations between successive dimers on the individual chains, but equivalent dimers (i.e., the zeroth, first, ..., or fifteenth) on all the chains are correlated in a manner analogous to Figure 4b. Such a model can be considered because of the separation of all the interference components in eq 11. It can be seen that, compared to the completely rigid structure, the maxima with even $h + k$ are weakened. Of course, in the real structure, even these limited correlations present problems in packing random sequences, but something like this is feasible given the possible nonlinearity of the chains and distortions of the bond angles. Insertion of further defects will probably result in elimination of the maxima with $h + k$ even, and such modifications are currently under consideration.

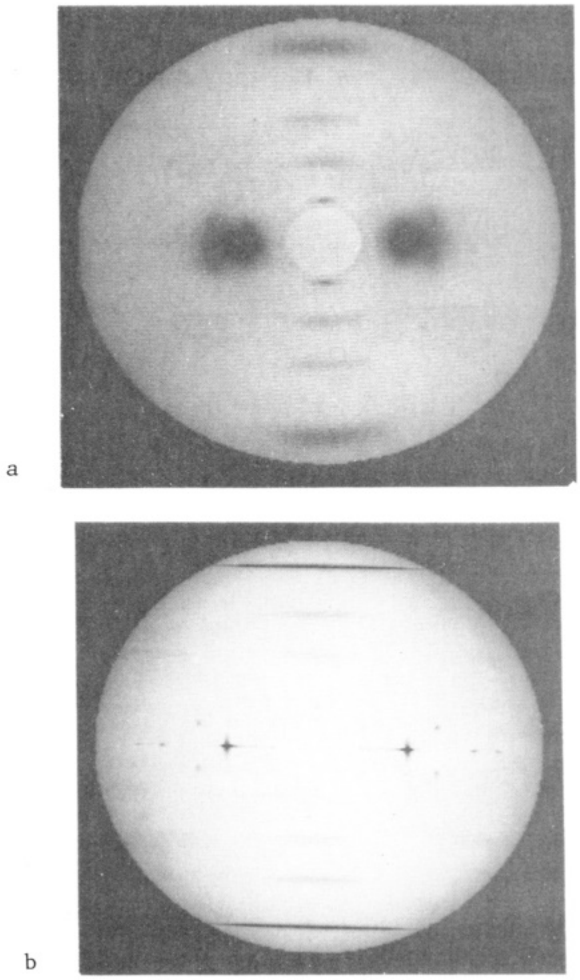

Figure 8. Comparison of (a) the composite fiber pattern for as-drawn 30/70 copoly(HBA/HNA) with (b) the composite calculated pattern derived for a structure with limited rotational correlations between chains and axial disorder corresponding to $\sigma = 2.0$ Å.

Figure 8 compares the fiber diffraction pattern for 30/70 copoly(HBA/HNA) with the observed data for as-spun samples. The latter data are a composite of the equator and first-layer line from a short exposure and the rest of the pattern from a longer exposure. The calculated data were derived for a structure in which rigid rotational correlations were limited to corresponding dimers on different chains. In addition, the condition for perfect registration of the origin ester oxygens was relaxed by using the $A(Z)$ axial disorder function. The standard deviation, σ, was set at 2.0 Å, following the results of paper 2,[6] where it was shown that this led to Bragg reflections on the first-layer line and continuous intensity on higher layer lines. It can be seen that there is reasonably good agreement between the observed and calculated data. Note that the observed data are in film space for a flat plate camera, whereas the calculated data are on a linear R,Z grid. No effort has been made to adjust the data for the effects of orientation.

The success of our model in predicting the observed Bragg maxima can be attributed to the presence of a high degree of local ordering of the aromatic groups. Previous calculations on the cylindrically averaged transforms of single "average" chains suggest that although strong conformational correlations exist between adjacent monomers, the entire chain by itself is not conformationally rigid; i.e., the random rotations between adjacent dimers are possible.[5] When such randomized chains are considered as an ensemble, several different factors which affect the extent of order in the entire system have to be considered. We have seen that the aperiodic meridional maxima arise as a consequence of monomer length correlations along the chain axis. Ordering such chains with their origins on a hexagonal lattice perpendicular to their axes results in the generation of additional lattice correlations not only in the lateral direction but also at other angles. It is the latter correlations that are responsible for the layer line reflections. Even in the absence of extensive lattice correlations, the highly anisotropic cross sections of the chains favor the formation of locally ordered regions where rigid rotational correlations are very likely to occur. In our model, we have assumed that rigid rotational correlations occur only between corresponding units on different chains. In physical terms, this implies that dimer unit m_i on chain i is in conformational register with the corresponding unit m_j on chain j but has no knowledge of the orientation of the preceding or succeeding dimer on the same chain or on neighboring chains. This situation could be visualized better in a layered structure where perfect packing order exists in each layer but no correlations exist between the layers. This situation cannot actually occur, since there will not be complete conformational freedom for successive dimers if they are also required to form layers with their axes on the same lattice, but a structure approximating this description is reasonable.

Further refinement of the structure via a point by point comparison of the calculated and observed data can be considered. Our analyses also need to be extended to consider factors such as chain sinuosity, chain disorientation, and defects in the packing arrangements, together with the gradual decay of correlations between adjacent units. Applicability of this model to other wholly aromatic liquid-crystalline copolymers is also in progress.

Acknowledgment. This research was supported by NSF Grant No. DMR84-17525 from the Polymer Program.

Registry No. (HBA)(HNA) (copolymer), 81843-52-9.

References and Notes

(1) Chivers, R. A.; Blackwell, J.; Gutierrez, G. A.; Stamatoff, J. B.; Yoon, H. In *Polymeric Liquid Crystals*; Blumstein, A., Ed.; Plenum: New York, 1985; p 153.
(2) Blackwell, J.; Gutierrez, G. A.; Chivers, R. A. *Macromolecules* **1984**, *17*, 1219.
(3) Blackwell, J.; Gutierrez, G. A.; Chivers, R. A.; Biswas, A. *J. Macromol. Sci., Phys.* **1985-1986**, *B24*(1-4), 39.
(4) Viney, C.; Windle, A. H. *J. Mater. Sci.* **1982**, *17*, 261.
(5) Biswas, A.; Blackwell, J. *Macromolecules*, companion paper in this issue.
(6) Biswas, A.; Blackwell, J. *Macromolecules*, companion paper in this issue.
(7) Blackwell, J.; Biswas, A.; Bonart, R. C. *Macromolecules* **1985**, *18*, 2126.
(8) Gutierrez, G. A.; Chivers, R. A.; Blackwell, J.; Stamatoff, J. B.; Yoon, H. *Polymer* **1983**, *24*, 937.
(9) Blackwell, J.; Biswas, A.; Gutierrez, G. A.; Chivers, R. A. *Faraday Discuss. Chem. Soc.* **1985**, *No. 79*, 73.
(10) Hanna, S.; Windle, A. H. *Polymer* **1988**, *29*, 207.
(11) Butzbach, G. D.; Wendorff, J. H.; Zimmermann, H. J. *Polymer* **1986**, *27*, 1337.
(12) Vainshtein, B. K. *Diffraction by Chain Molecules*; Elsevier: Amsterdam, 1966; p 269.
(13) Geiss, R. H.; Street, G. B.; Volksen, W.; Economy, J. *IBM J. Res. Dev.* **1983**, *27*(4), 321.
(14) Northolt, M. S. *Eur. Polym. J.* **1974**, *10*, 799.
(15) Blackwell, J.; Cheng, H.-M.; Biswas, A. *Macromolecules* **1988**, *21*, 39.

Characterization of Ethylene Copolymers with ^{1}H NMR Techniques and Reaction Probability Models[1]

H. N. Cheng*

Hercules Incorporated, Research Center, Wilmington, Delaware 19894

G. H. Lee*

Sun Refining and Marketing Company, P.O. Box 1135, Marcus Hook, Pennsylvania 19061.

Received November 20, 1987

ABSTRACT: Complete ^{1}H NMR spectral analysis is carried out for ethylene–vinyl chloride, ethylene–vinyl alcohol, and ethylene–vinyl acetate copolymers. Three approaches (two-dimensional NMR, empirical shift rules, and computerized "analytical" method) have been used in concert to provide detailed ^{1}H spectral assignments and quantitative analysis. It is shown that the use of these three approaches permits detailed compositional and comonomer sequence information to be obtained from high-field ^{1}H NMR spectra.

Introduction

Nuclear magnetic resonance (NMR) spectroscopy has been firmly established as a primary technique for polymer analysis.[2-6] Beginning with ^{1}H NMR in the 1960s and continuing with ^{13}C in the 1970s, NMR has been used to study innumerable polymer systems, with generally excellent results. In recent years ^{13}C NMR has mostly displaced ^{1}H in studies of polymer microstructure. Because of its larger chemical shift range, ^{13}C NMR provides more detailed structural information. Although less popular for polymers, ^{1}H NMR has the advantage of higher sensitivity and relative ease in quantitation. It would be desirable to obtain equivalent information from ^{1}H NMR polymer spectra.

The steps in the use of ^{1}H NMR for problem solving can be depicted as follows:

$$\text{spectral data} \rightarrow \text{spectral interpretation} \rightarrow \text{spectral analysis} \rightarrow \text{structure}$$

Usually one starts by obtaining the ^{1}H NMR spectrum, assigns the resonances (frequently with the help of spectral libraries and known chemical shifts), analyzes the spectrum (e.g., with computational schemes involving selected spectral intensities), and obtains the result. Since one begins with the NMR spectrum and analyzes it, this can be called the "analytical approach".[7,8] [The reverse process, called "synthetic approach", has also been proposed.[9,10]] In many polymers, both the spectral interpretation and the spectral analysis pose problems. The ^{1}H resonances corresponding to different polymer microstructures are often severely overlapped. Because of the small ^{1}H chemical shift range (12 ppm), only in a few cases can sequence determinations be carried out beyond the triad level.[6] The use of high-frequency spectrometers mitigates the problem to some extent but does not eliminate it.

Quite a few techniques have been developed over the years to sidestep these difficulties. For example, deuteriation,[2] solvent shifts,[2] two-dimensional (2D) NMR techniques,[11-28] lanthanide shift reagents,[28-34] and empirical additive shift rules[35] have been used to facilitate spectral

0024-9297/88/2221-3164$01.50/0